OsteoArthritis and Cartilage (2006) **14,** 967–973

doi:10.1016/j.joca.2006.03.017

Osteoarthritis and Cartilage

International Cartilage Repair Society

OARSI OSTEOARTHRITIS RESEARCH SOCIETY INTERNATIONAL

MR measurement of articular cartilage thickness distribution in the hip

Dr J. H. Naish Ph.D.†*, Dr E. Xanthopoulos Ph.D.†, Dr C. E. Hutchinson M.D., F.R.C.R.†, Dr J. C. Waterton Ph.D.‡ and Prof C. J. Taylor Ph.D.†

† *Imaging Science and Biomedical Engineering, University of Manchester, Stopford Building, Oxford Road, Manchester, M13 9PT, UK*

‡ *Global Sciences and Information, AstraZeneca, Alderley Park, Macclesfield, Cheshire, SK10 4TG, UK*

Summary

Objective: To develop a method to determine the distribution of articular cartilage in the hip and to evaluate the potential of the method in a study of normal weight-bearing effects in asymptomatic young volunteers.

Design: Six volunteers were scanned after periods of standing and lying supine, using 3D gradient-echo magnetic resonance imaging (MRI). The protocol was repeated for two successive weeks to determine reproducibility. The femoral and acetabular cartilage layers were segmented as a single unit and thickness distribution maps were calculated using a spherical bone model as a frame of reference. Thickness maps were combined over the population using the bone model and post-weight-bearing and post-resting maps were compared.

Results: Mean thickness values were compared using an analysis of variance and a significant increase in cartilage thickness of 0.05 mm ($P = 0.02$) was observed. The reproducibility of the method, assessed using test–retest coefficient of variation was 2.5%.

Conclusions: The technique is reproducible, sensitive to sub-millimetre changes in thickness and may be useful in monitoring changes due to disease progression in patients with arthritis of the hip.

Key words: Cartilage, Hip, Thickness, Weight-bearing.

Introduction

There has been considerable interest in recent years in developing quantitative magnetic resonance imaging (MRI) methods to assess articular cartilage in the knee. Much of this has been driven by a need for new biomarkers of osteoarthritis (OA) for use in longitudinal trials of potential new therapies. Accurate and reproducible measurements of both volume and thickness of knee cartilage have been presented using high resolution 3D gradient-echo imaging with fat suppression[1–3] and have been shown to be useful in monitoring disease progression[4,5]. Changes in total cartilage volume are small in OA, however, and increasingly studies have concentrated on developing techniques for mapping cartilage thickness in order to investigate local changes[6–9].

Despite the major advances in quantitative magnetic resonance (MR) assessment of knee cartilage there is currently little in the literature on quantification of hip volume or thickness from MRI. McGibbon *et al.* have reported measurements of acetabular[10] and femoral[11] cartilage thickness *in vitro* but to our knowledge the only *in vivo* studies have been performed by Nishii *et al.*[12–14]. MR assessment of the cartilage of the hip is more challenging than that of the knee. The MR resolution, which can be achieved in a reasonable time and with adequate signal-to-noise is lower because the location of the hip requires the use of surface coils. The spherical morphology of the joint leads to partial volume averaging in the highly curved articular cartilage surface. The joint space width is much narrower in the hip compared with the knee making it difficult to separate the cartilage on opposing articulating bone surfaces. This problem was overcome in the work of Nishii *et al.* by the use of continuous leg traction.

The main objective of this study was to develop a technique for producing cartilage thickness maps from MR images that can be applied to the hip and that will allow comparison across populations and in longitudinal studies. The method we have developed uses the bone surface to define a common reference frame. In this study we have used the method to measure the effect of normal weight-bearing on the distribution of cartilage in the hips of asymptomatic young female adults. The study represents a first step towards developing hip cartilage thickness mapping as a potential biomarker of OA.

Methods

SUBJECTS AND STUDY PROTOCOL

Six female volunteers aged 22–34, without symptoms or history of any hip disorder were recruited for the study. Local research ethical committee approval was obtained prior to scanning and the volunteers gave informed consent. Before each scan session commenced, the subjects were asked to remain standing (or walking) for at least 1 h. The subjects were then placed in the scanner supine, secured in position with foam padding and with the feet turned inwards and tied together to obtain a reproducible orientation

*Address correspondence and reprint requests to: Dr Josephine Helen Naish, Ph.D., Imaging Science and Biomedical Engineering, University of Manchester, Stopford Building, Oxford Road, Manchester, M13 9PT, UK. Tel: 44-0-161-2756871; Fax: 44-0-161-2755145; E-mail: josephine.naish@manchester.ac.uk
Received 10 October 2005; revision accepted 28 March 2006.

of the joint and to minimise movement during the scan. Two 3D gradient-echo images were acquired. The first, optimised for good cartilage delineation, took 11 min 11 s and was acquired immediately following initial scanner set up and scout scan. The second, optimised for good visualisation of the bone surface, took 8 min 54 s. The total time inside the scanner was approximately 35 min. Subjects were then lifted onto a trolley and remained supine outside the scanner for a further 35 min (total time supine: 1 h 10 min) before being returned to the scanner for a second scan session. The protocol was repeated a week later at the same time of day so that a total of four complete sets of images were acquired for each subject.

MRI PROTOCOL

Imaging was carried out using a 1.5 T Philips Gyroscan NT Integra MR System (Philips Medical Systems, Best, Netherlands). Two sets of 3D gradient-echo images of the right hip were taken oriented with the slices in an oblique sagittal direction. This slice orientation was chosen to be perpendicular to the cartilage in the region most likely to be affected by weight-bearing in order to minimise partial volume averaging in this region. The first acquisition used a fat-suppressed, T_1-weighted sequence (repetition time (TR) = 58 ms, echo time (TE) = 11 ms, 40° flip angle), which provides a good contrast between the cartilage and surrounding tissue. These images allowed a semi-automatic segmentation of the hip articular cartilage. The second acquisition used a T_2-weighted sequence (TR = 15.4 ms, TE = 5.9 ms, 25° flip angle), with no suppression. This sequence produces images which allow the edge of the bone to be identified for use as a common frame of reference. Both image sets had an in-plane resolution of 0.78 mm, a slice thickness of 1.6 mm and covered an identical field of view resulting in corresponding image slices. Example corresponding slices from the two imaging protocols are illustrated in Fig. 1.

IMAGE SEGMENTATION

Image segmentation was carried out to sub-voxel accuracy using a semi-automated method based on the livewire algorithm[15] implemented in the software package Endpoint (imorphics, Manchester, UK). This algorithm has been shown recently to produce accurate and reproducible segmentation of cartilage[16] and the method is considerably faster than manual segmentation; typically a single image set was segmented in under 1 h. The intra-observer coefficient of variation (CoV) for volume of knee cartilage obtained by segmentation using the Endpoint package has previously been measured at 1.8% (JCW, data not presented here). All segmentations were performed blinded to weight-bearing status and visit date, but not to patient ID.

The upper section of the femur was segmented on a slice-by-slice basis from the T_2-weighted images. It was not possible to distinguish the acetabular and femoral cartilage layers on the fat-suppressed T_1-weighted images due to the narrow joint space width and adhesive nature of the two layers at the weight-bearing area[14], so the entire cartilage of the hip was segmented as a single unit.

DATA ANALYSIS

A simple geometric model was fitted to the bone segmentation in order to define a common coordinate system. A sphere was fitted to the femoral head using a Gauss–Newton least squares routine[17]. The centre of the sphere provided the origin of a common reference frame, and the radius of the sphere was used as the scaling factor. A direction was provided by the shaft of the femur. Only the upper end of the shaft is visible in the images, and this was found to be most simply represented by a conic section. The axis of the cone together with the centre of the sphere was used to define a plane, which in turn defined the meridian of a unique coordinate system. An example bone segmentation together with the corresponding sphere-plus-cone fit is illustrated in Fig. 2.

Cartilage thickness maps were produced for each individual data set using the following steps. First, a surface was constructed from the cartilage segmentation using the method of Williams *et al.*[9]. In this method, inner and outer cartilage surfaces are identified for each segment and the segments are then connected. The operation is automated, with manual correction to the labelling and/or connections if required. The resulting quadrilateral mesh is triangulated to generate inner and outer surfaces. Equally spaced points were defined on the surface of a unit sphere by tessellation and mapped into the image coordinate system using the bone model fit parameters. Cartilage

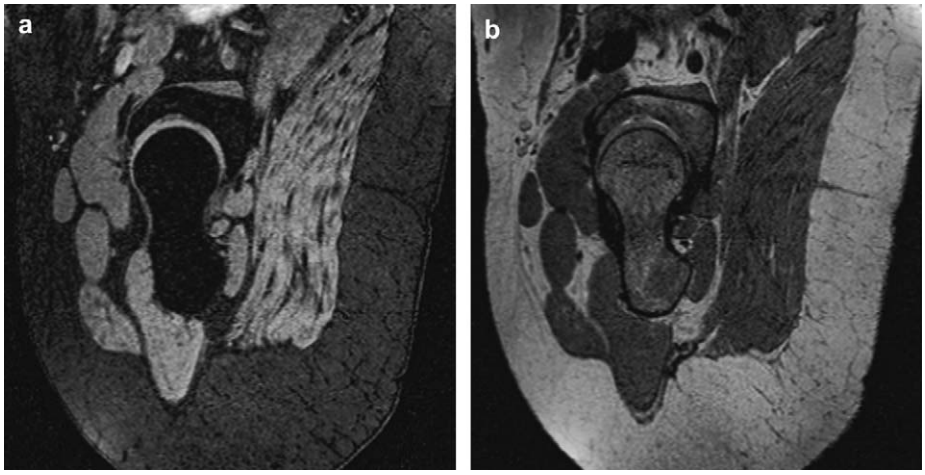

Fig. 1. Corresponding oblique sagittal slices from 3D MR image sets of the right hip using (a) a fat-suppressed 3D gradient echo and (b) a T_2-weighted 3D gradient-echo sequence.

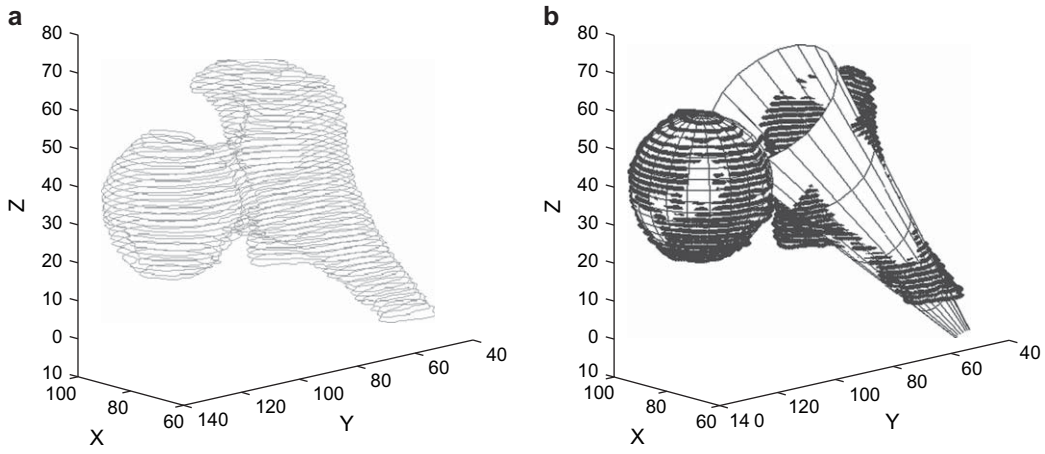

Fig. 2. (a) A typical bone segmentation and (b) the results of a fit of a sphere-plus-cone model to the bone segmentation.

thickness measurements were made along radial lines passing through these points by finding the intersection with the faces of the inner and outer cartilage surfaces. The set of thickness values was then mapped back onto the unit sphere to produce a cartilage thickness map in the common reference frame.

Cartilage thickness maps were combined across individuals and visits to produce population mean thickness maps for the post-weight-bearing and the post-resting cases. Thickness difference maps (post-resting minus post-weight-bearing) were calculated for each individual at each visit and these were also combined across individuals and visits to produce a single population mean thickness difference map.

Mean cartilage thickness values were calculated for each individual data set by spatial averaging across each thickness map.

STATISTICAL ANALYSIS AND REPRODUCIBILITY

Mean cartilage thickness values were compared using a repeated measures analysis of variance (ANOVA), with weight-bearing status and visit date as the repeated measures.

The overall reproducibility of the method was assessed using the test–retest CoV of the mean thickness values. For each subject, i, the CoV is defined as the standard deviation of a series of measurements, σ_i, divided by the mean, μ_i and expressed as a percentage. The overall CoV for a group of N subjects is the root mean square average of the subject CoVs.

Test–retest CoV was also calculated separately for the post-weight-bearing and post-resting cases. To test for a significant difference in reproducibility between the two cases, the log ratio of the measurement at visit 1 to that at visit 2 was calculated for each, and a linear regression of the sum of the log ratios on the difference of the log ratios was performed. A test of whether there is a significant correlation in this model is equivalent to a testing for a significant difference in reproducibility[18].

Results

THICKNESS MAPS

An example cartilage thickness map, displayed superimposed on the unit sphere in the common reference frame, is presented in Fig. 3. The medial view of the map is displayed in Fig. 3(a) and this is also shown to be superimposed onto the bone segmentation in Fig. 3(b) as an aid to the viewer in orientation. The map represents the entire cartilage of the hip with the acetabular cartilage superimposed onto the femoral. The hole in the cartilage corresponds to the fovea on the head of the femur for the attachment of the ligament. Population mean thickness maps for post-weight-bearing and post-resting are presented in Fig. 4. The horseshoe shaped thicker region of cartilage corresponding to the acetabular cartilage superimposed onto the femoral cartilage can be seen more clearly in the population-averaged maps. The cartilage appears to be thicker in the anterior region and has a thinner area superiorly, corresponding to the region of weight-bearing. The most obvious difference visually between the mean post-weight-bearing and post-resting thickness maps is in this superior region, central to the horseshoe of acetabular cartilage, which appears to thicken following the period of resting. This observation is confirmed in the mean difference map in Fig. 4(c) which shows a region of thickening anteriosuperiorly.

GLOBAL MEASURES

Mean thickness values across the cartilage surface for each individual for post-weight-bearing and post-resting are summarised in Table I and plotted in Fig. 5. In nine out of 12 (2 visits $\times$ 6 subjects) cases the mean cartilage thickness increased following the period of non-weight-bearing. The average global change was $+0.05 \pm 0.05$ mm. The ANOVA (Table II) showed that this increase was statistically significant ($P < 0.02$). There was no significant change in thickness due to visit date.

The reproducibility of the method, expressed as the overall test–retest CoV, was 2.5%. The test–retest CoV for the post-weight-bearing case was 3.1% and for the post-resting case was 1.7%. The linear regression of the sum of the log ratios, i.e., log(mean_thickness_at_visit_1/mean_thickness_at_visit_2) for the post-weight-bearing and post-resting measurements, on the difference of the log ratios showed a positive correlation between the two parameters ($R^2 = 0.47$). This trend towards a difference in CoV was not statistically significant ($P = 0.12$), but tends to suggest that the reproducibility of the method post-weight-bearing may be slightly worse than the reproducibility of post-resting.

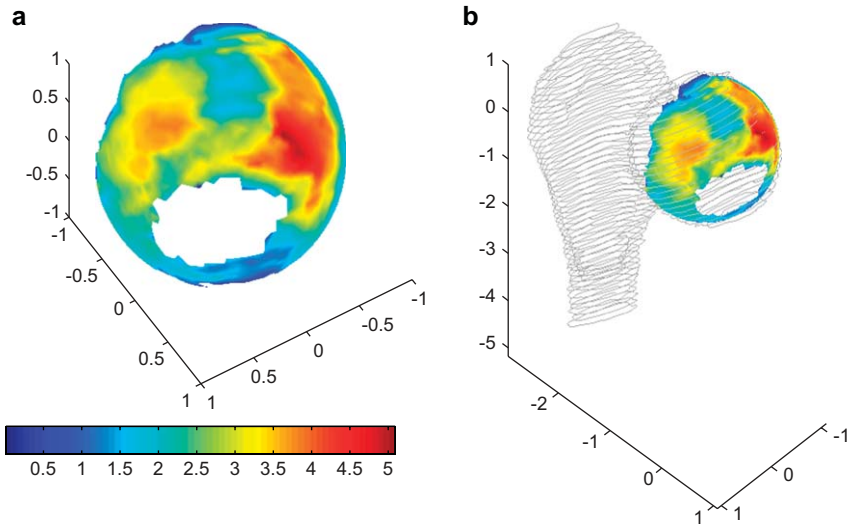

Fig. 3. (a) Medial view of an example cartilage thickness map for one of the subjects calculated from MR data taken post-weight-bearing, displayed in the normalised common reference frame. The colour scale is in millimetres. In (b), the map is shown superimposed onto the corresponding transformed bone segmentation as an aid to orientation.

Discussion

We have presented a method to produce hip cartilage thickness maps and combine them across a population. The head of the femur is approximately spherical in shape, allowing a simple geometric model to be used. The cone fit to the upper section of the shaft of the femur defines a direction. The fitting is simple with minimal user input; it does not require manual definition of anatomical landmarks. In the group of normal volunteers studied, the method aligns the cartilage well between subjects and scan sessions, as evidenced by the alignment of the fovea in the cartilage thickness maps. We have yet to test the method in OA patients.

Unlike the knee, in which separate cartilage compartments are easily identified on an MR image, the hip has a very narrow joint space and the acetabular and femoral cartilage layers cannot easily be distinguished. Previous authors used continuous leg traction to separate the cartilage layers. This works well, but may be unacceptable to OA patients for the purpose of longitudinal studies and the traction force may itself affect the cartilage thickness distribution. In the present study a different approach was adopted in which the entire cartilage of the joint was segmented as a single unit. The disadvantage of this approach is that it is not possible to locate changes in thickness to particular cartilage compartment, although an overall change in thickness still provides a useful marker of disease progression. It is also more prone to relative repositioning errors, which can be overcome to a certain extent by careful positioning of the subject. Both of these disadvantages are present in the current gold standard used to monitor progression of OA in the hip, which is the joint space as measured on a plain radiograph[19]. Differences in the relative positioning of the acetabular and femoral cartilage layers between subjects may also lead to errors when combining maps over a population and these errors may be larger in a patient population.

The population mean thickness maps provide a direct visualisation of the distribution of cartilage in the hip. Further

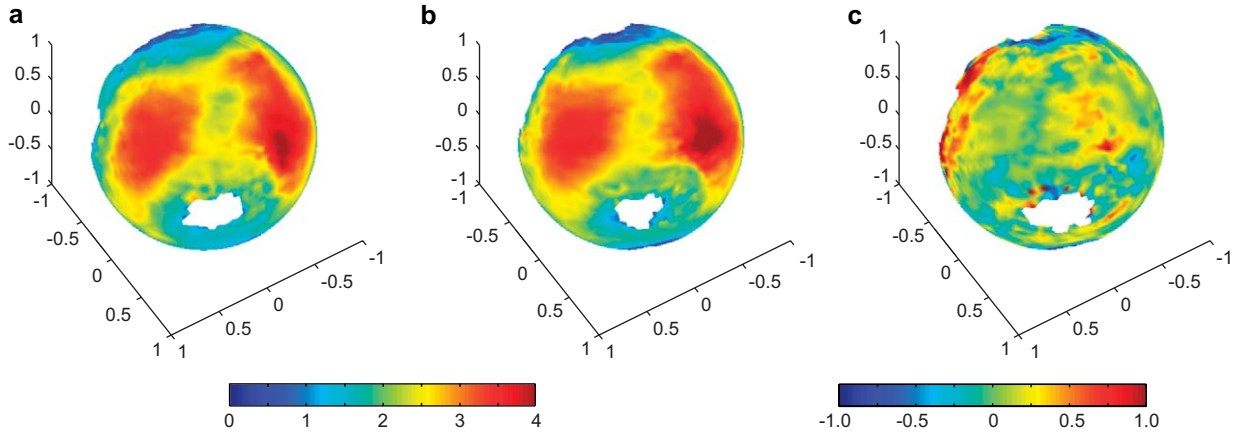

Fig. 4. Population-averaged thickness maps for (a) post-weight-bearing and (b) post-resting, medial view, displayed in the normalised common reference frame. (c) Population-averaged thickness difference map (post-resting minus post-weight-bearing). Colour scales are in millimetres.

Table I
Mean cartilage thickness values in millimetres for each individual data set, calculated by spatial averaging across each thickness map

Subject	Visit	Cartilage thickness, post-weight-bearing (mm)		Cartilage thickness, post-resting (mm)	
		Mean	sd	Mean	sd
1	1	2.32	0.89	2.39	0.92
	2	2.27	0.86	2.41	0.9
2	1	2.43	1.06	2.53	1.12
	2	2.36	0.96	2.43	1.06
3	1	2.5	0.88	2.46	0.92
	2	2.34	0.86	2.39	0.91
4	1	2.09	0.71	2.14	0.73
	2	2.22	0.69	2.2	0.72
5	1	2.32	0.98	2.43	0.92
	2	2.43	0.98	2.42	0.94
6	1	2.13	0.67	2.18	0.78
	2	2.12	0.66	2.2	0.67

work is required to evaluate and further develop the technique in order to produce population thickness maps across an OA population. These maps may be useful in future studies of hip OA, both to compare overall thickness distributions for normals and OA patients to identify regional effects of disease, and in longitudinal studies of progression and/or therapeutic intervention. The population mean thickness maps produced are consistent with a femoral articular cartilage layer with a horseshoe region of acetabular cartilage overlaid. The local mean thicknesses are consistent with *in vitro* measurements of cartilage thickness[20,21] except in the thinner superior region. This may be due to compression of the cartilage *in vivo* in the weight-bearing area. The overall mean cartilage thickness was 2.3 ± 0.13 mm which is not inconsistent with *in vitro* measurements, e.g., Adam *et al.*[21] quote a mean thickness of 1.3 ± 0.17 mm for the separate femoral and acetabular cartilage compartments. Changes in the thickness distribution as a result of unloading can be seen by directly comparing the population mean thickness maps in Fig. 4(a and b). The main difference is the anteriosuperior region and corresponds to the region in which maximum contact pressure has been observed in biomechanical studies[22], i.e., to the region of maximum weight-bearing. Examination of the difference map [Fig. 4(c)] reveals some regions of large change (positive and negative) around the outer edges of the femoral cartilage. These are likely to be artifactual, due to partial volume errors in those regions where the angle between the cartilage surface and the imaging plane is small, and due to segmentation errors in determining the extent of the cartilage around the head of the femur. Partial volume errors may be reduced by reducing the slice thickness although to retain sufficient signal-to-noise it may be necessary to scan at higher fields. In the present study, the slice orientation was chosen to be oblique sagittal so that the cartilage surface was perpendicular to the imaging plane in the regions of maximum weight-bearing.

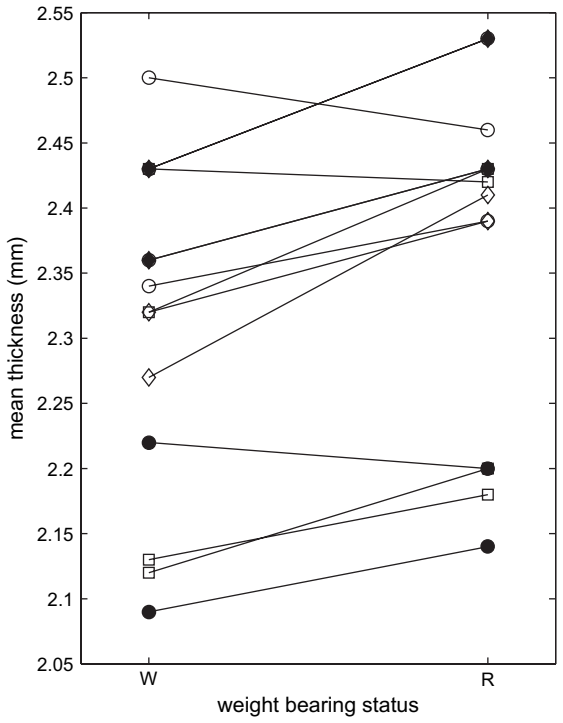

Fig. 5. Mean cartilage thickness values for each individual for post-weight-bearing (W) and post-resting (R) for each of the two visits. The different symbols indicate different individuals.

The statistical analysis of the spatially averaged cartilage thicknesses showed that the difference observed due to weight-bearing was significant at a 2% level. The average was taken over the whole cartilage surface but for improved statistical power in an OA study it may be preferable to define *a priori* anatomical regions of interest. In young adults, unloading increases height by about 17 mm[23] with 41% of this change occurring in the first hour recumbent. Most of this variation arises from the compression of the cartilage in the invertebral discs, but the articular cartilage in the knee[7], and no doubt ankle, also contributes as well as the hip (as shown for the first time in this study). Liess *et al.*[24] measured significant increases in the thickness of patellar cartilage between images taken immediately after knee bend exercise and after 45 min of rest. The tiny changes in the hip were only detectable because of the averaging across anatomical regions, subjects and visits enabled by our technique. It should also be noted that degenerate cartilage responds differently to unloading, so our method may also provide an index of cartilage quality.

Since cartilage is lost relatively slowly in OA, a technique with adequate reproducibility is required to monitor OA disease progression. The reproducibility of our method in normal volunteers, as measured by the test–retest CoV, was 2.5%, which compares well with values quoted in similar studies of the knee[5]. Further studies in a patient population

Table II
Summary statistics

Two-way repeated measures ANOVA				
Source	Sum of squares	Mean sq	*F*	*P*
Visit (V)	0.0007	0.0007	0.1117	0.7
Weight-bearing status (W)	0.0176	0.0176	11.55	0.019
V × W	0.00004	0.00004	0.0221	0.9
Test–retest CoV				
Weight-bearing				3.1%
Resting				1.7%
Overall				2.5%

are required to determine the reproducibility when changes due to disease are present. The ability to detect the small changes in thickness due to weight-bearing is an indication of the sensitivity of the technique but this also highlights a potentially confounding factor in OA studies. The reproducibility of the measurements taken post-resting was 1.7% compared to 3.1% for the post-weight-bearing measurements. Although this trend was not statistically significant we suggest that it may be advisable to include a period of non-weight-bearing immediately prior to scanning in a longitudinal OA study.

There are a number of shortcomings in the present study. This was intended as a proof of concept using a relatively small number of normal volunteers. Further studies, both in volunteers and in patients, will be required to develop and refine the method. The MR image resolution is less than ideal because of the relative size of the joint compared to the imaging coil. This problem may be exacerbated in OA studies, which often involve patients with a high body mass index. To achieve acceptable signal-to-noise in a reasonable time we opted for anisotropic voxels so maximising the image resolution perpendicular to the cartilage in the anatomical regions most of interest. In the future it may be desirable to image using higher fields to improve resolution and we are currently investigating imaging the hip at 3 T. A related problem is the inability to separate the cartilage layers. While we were still able to make useful measurements using an aggregate cartilage thickness in healthy volunteers, it remains to be seen whether the errors in repositioning become too large when dealing with OA patients in a longitudinal study in which disease progression may change the alignment of the joint.

This study was motivated by a requirement for new biomarkers of OA, which could be utilised in longitudinal studies of potential new treatments. However, the techniques that we have developed have a number of other potential applications, for example, in studying changes in cartilage thickness associated with loading changes through the joint as a result of osteotomy, ipsilateral joint replacement, or back surgery. The technique could potentially be of benefit in confirming the biomechanical models of joint loading and how these alter cartilage loading (thickness) after such treatments.

In conclusion, we have presented a technique to produce sensitive and reproducible measurements of hip articular cartilage thickness. The technique allows thickness distribution maps to be combined over populations and/or in longitudinal studies. A statistically significant increase in hip cartilage thickness was observed as a result of removal of weight-bearing. This increase tended to be localised in a region expected to correspond to the region of maximum weight-bearing contact pressure. With further development, the technique may be useful in both population and longitudinal studies of OA of the hip.

References

1. Peterfy CG, van Dijke CF, Janzen DL, Gluer CC, Namba R, Majumdar S, *et al*. Quantification of articular cartilage in the knee with pulsed saturation transfer subtraction and fat-suppressed MR imaging: optimization and validation. Radiology 1994;192:485–91.
2. Stammberger T, Eckstein F, Englmeier KH, Reiser M. Determination of 3D cartilage thickness data from MR imaging: computational method and reproducibility in the living. Magn Reson Med 1999;41:529–36.
3. Glaser C, Faber S, Eckstein F, Fischer H, Springer V, Heudorfer L, *et al*. Optimization and validation of a rapid high-resolution T1-w 3D FLASH water excitation MRI sequence for the quantitative assessment of articular cartilage volume and thickness. Magn Reson Imaging 2001;19:177–85.
4. Wluka AE, Stuckey S, Snaddon J, Cicuttini FM. The determinants of change in tibial cartilage volume in osteoarthritic knees. Arthritis Rheum 2002;46:2065–72.
5. Eckstein F, Cicuttini F, Raynauld JP, Waterton JC, Peterfy CG. Magnetic resonance imaging (MRI) of articular cartilage in knee osteoarthritis (OA): morphological assessment. Osteoarthritis Cartilage (in press).
6. Stammberger T, Hohe J, Englmeier KH, Reiser M, Eckstein F. Elastic registration of 3D cartilage surfaces from MR image data for detecting local changes in cartilage thickness. Magn Reson Med 2000;44: 592–601.
7. Waterton JC, Solloway S, Foster JE, Keen MC, Gandy S, Middleton BJ, *et al*. Diurnal variation in the femoral articular cartilage of the knee in young adult humans. Magn Reson Med 2000;43:126–32.
8. Cohen ZA, Mow VC, Henry JH, Levine WN, Ateshian GA. Templates of the cartilage layers of the patellofemoral joint and their use in the assessment of osteoarthritic cartilage damage. Osteoarthritis Cartilage 2003;11:569–79.
9. Williams TG, Taylor CJ, Gao ZX, Waterton JC. Corresponding articular cartilage thickness measurements in the knee joint by modelling the underlying bone, Medical Image Computing and Computer-Assisted Intervention – Miccai 2003, Pt 2. In: Lecture Notes in Computer Science 2003; Volume 2879:480–7.
10. McGibbon CA, Dupuy DE, Palmer WE, Krebs DE. Cartilage and subchondral bone thickness distribution with MR imaging. Acad Radiol 1998;5:20–5.
11. McGibbon CA, Bencardino J, Yeh ED, Palmer WE. Accuracy of cartilage and subchondral bone spatial thickness distribution from MRI. J Magn Reson Imaging 2003;17:703–15.
12. Nishii T, Sugano N, Sato Y, Tanaka H, Miki H, Yoshikawa H. Three-dimensional distribution of acetabular cartilage thickness in patients with hip dysplasia: a fully automated computational analysis of MR imaging. Osteoarthritis Cartilage 2004;12:650–7.
13. Nakanishi K, Tanaka H, Nishii T, Masuhara K, Narumi Y, Nakamura H. MR evaluation of the articular cartilage of the femoral head during traction. Correlation with resected femoral head. Acta Radiol 1999; 40:60–3.
14. Nishii T, Nakanishi K, Sugano N, Masuhara K, Ohzono K, Ochi T. Articular cartilage evaluation in osteoarthritis of the hip with MR imaging under continuous leg traction. Magn Reson Imaging 1998;16: 871–5.
15. Barrett WA, Mortensen EN. Fast, accurate, and reproducible live-wire boundary extraction, Visualization in Biomedical Computing. In: Lecture Notes in Computer Science 1996; Volume 1131:183–92.
16. Gougoutas AJ, Wheaton AJ, Borthakur A, Shapiro EM, Kneeland JB, Udupa JK, *et al*. Cartilage volume quantification via live wire segmentation. Acad Radiol 2004; 11:1389–95.
17. Roach JW, Hobatho MC, Baker KJ, Ashman RB. Three-dimensional computer analysis of complex acetabular insufficiency. J Pediatr Orthop 1997;17: 158–64.

18. Armitage B, Berry G, Matthews J. Statistical Methods in Medical Research. Blackwell Science 2002;203–4.
19. Dougados M, Nguyen M, Berdah L, Mazieres B, Vignon E, Lequesne M. Evaluation of the structure-modifying effects of diacerein in hip osteoarthritis: ECHODIAH, a three-year, placebo-controlled trial. Evaluation of the chondromodulating effect of diacerein in OA of the hip. Arthritis Rheum 2001;44: 2539–47.
20. Kurrat HJ, Oberlander W. The thickness of the cartilage in the hip joint. J Anat 1978;126:145–55.
21. Adam C, Eckstein F, Milz S, Putz R. The distribution of cartilage thickness within the joints of the lower limb of elderly individuals. J Anat 1998;193(Pt 2):203–14.
22. Afoke NY, Byers PD, Hutton WC. Contact pressures in the human hip joint. J Bone Joint Surg Br 1987;69:536–41.
23. Krag MH, Cohen MC, Haugh LD, Pope MH. Body height change during upright and recumbent posture. Spine 1990;15:202–7.
24. Liess C, Lusse S, Karger N, Heller M, Gluer CC. Detection of changes in cartilage water content using MRI T2-mapping *in vivo*. Osteoarthritis Cartilage 2002;10:907–13.